LOCAL PARAMETRIZATIONS VIA LAPLACIAN EIGENFUNCTIONS

MADELEINE R UDELL

Abstract. Eigenfunction methods for mapping high dimensional data sets into lower dimensional spaces are useful in a broad range of applications. In particular, a recent paper by Jones et al [2] shows that eigenfunctions of the Laplacian operator give a good local coordinate system under very general conditions. Here I outline the proof of the theorem and explore its use in cryo-electron microscopy.

1. Introduction

The problem of mapping data from a high dimensional space into a lower dimensional space occurs frequently in all manner of scientific application. Examples include visualizing high dimensional data in 3D, finding the path a protein takes as it unfolds, and discovering the shape of a molecule using cryo-electron microscopy.

The central idea of this paper is that one can often use the eigenfunctions of the Laplacian to perform this mapping. The theoretical basis for this method is the theorem due to Jones et al [2] (Theorems 2.1.1 and 2.2.1) that states that under very general conditions, one can find a set of Laplacian eigenfunctions to map a local region of a Euclidean domain or of a manifold onto $\mathbb{R}^d$ with low distortion. More precisely,

Theorem 1. *given a finite volume manifold $\mathcal{M}$ with metric, and a point $z \in \mathcal{M}$ of local dimension d, there exists a constant κ that depends only on the dimension of the manifold and properties of its metric such that for any ρ smaller than the distance from z to the boundary of the manifold, one can find a set of d eigenfunctions of the Laplacian that can be used to map a local ball $B(z, \kappa^{-1}\rho)$ into $\mathbb{R}^d$ with low distortion. That is, we can find a map*

$$\Phi : B(z, \kappa^{-1}\rho) \to \mathbb{R}^d \tag{1.1}$$

$$x \mapsto (\gamma_1 \phi_{i_1}(x), \ldots, \gamma_d \phi_{i_d}(x))$$

for suitable set of coefficients

$$\gamma_l = \frac{1}{\mid B(z, \kappa^{-1}\rho) \mid} \left(\int_{B(z,\kappa^{-1}\rho)} \phi_{i_l}^2 \right)^{-\frac{1}{2}} \tag{1.2}$$

such that the distortion is bounded for any $x_1, x_2 \in B(z, \kappa^{-1}\rho)$:

$$\frac{\kappa^{-1}}{\rho} \|x_1 - x_2\| \leq \|\Phi(x_1) - \Phi(x_2)\| \leq \frac{\kappa}{\rho} \|x_1 - x_2\| \tag{1.3}$$

To my advisor, Peter Jones, and to Yoel Shkolnisky for discussion of the cryo-EM application.

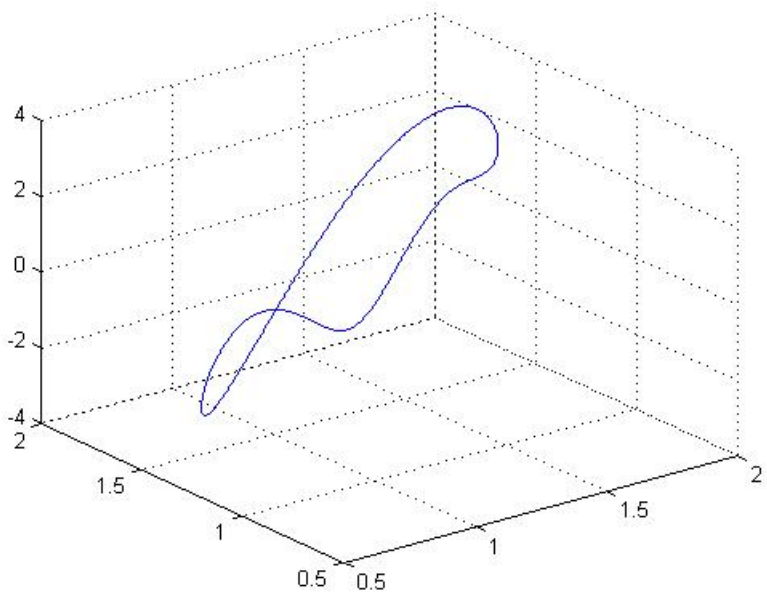

FIGURE 2.1. A distorted circle in $\mathbb{R}^3$

Furthermore, these eigenfunctions can be chosen such that their eigenvalues satisfy

$$\kappa^{-1}\rho^{-2} \leq \lambda_{i_1}, \ldots, \lambda_{i_d} \leq \kappa\rho^{-2}$$

This constraint on the eigenvalues is what makes this theorem useful in practice. For while on any given data set we cannot compute the eigenfunctions of the (continuous) Laplacian operator, we can often compute the eigenvectors of a discrete operator whose eigenvectors converge to the eigenfunctions of the Laplacian so long as the eigenvalues are within a bounded range. Note that this theorem is only an existence theorem: it does not mean that the search for these eigenfunctions will be easy.

The first section of this paper demonstrates how the laplacian eigenfunction maps work on simple discrete examples, emphasizing the connection between the graph laplacian and its continuous counterpart. The second section of the paper explores in greater detail the use of the method in analyzing data from cryo-electron microscopy. The third section presents the idea of the proof of the theorem stated above. Appendices include relevant proofs (spectral, Weyl, CLT).

2. Some simple examples

2.1. **The circle.** Consider the case of a circle. But no simple, garden-variety circle-in-$\mathbb{R}^2$: suppose this circle is embedded in a much higher dimensional space. How can we map the points on this strange circle back to an ordinary circle in two dimensions?

Let's frame the problem in a way that it might emerge in an experimental context. For example, the data might be the coordinates of the n amino acids in a protein

as the protein undergoes a cyclic folding/unfolding cycle. As time proceeds, the coordinates of the data points should trace out a closed loop through $\mathbb{R}^{3n}$. Suppose we know that the data points were taken at equal time intervals, but that we don't know which picture corresponds to which time.

The philosophy of this paper would tell us to proceed as follows. On our data set, we can construct a graph laplacian L (the use of the term "laplacian" for this beast will be justified later, or see appendix A.4) as follows:

$$L_{ij} = \begin{cases} \frac{1}{|\mathcal{N}(j)|} : & i \in \mathcal{N}(j) \\ 0 : & i \notin \mathcal{N}(j) \end{cases}$$

where $i \in N(j)$ if i is a neighbor of j. In the case of the circle, i is a neighbor of j if it comes immediately before or after j along the path of the circle through $\mathbb{R}^{3n}$. The theorem tells us that (if we can believe that this graph laplacian works like the real Laplacian) that there exists an eigenvector that can map regions of this circle back onto $\mathbb{R}^1$ with low distortion. So we could just plug this matrix into Matlab, find the eigenvectors, and try each one to see how it does on distortion. But it behooves us to try thinking about what we expect the eigenvectors to look like.

Let's suppose we have m points, so that L is an $m \times m$ matrix. The trivial eigenvector is the easiest to understand. This is the eigenvector consisting entirely of ones: $\vec{1}$. Since each row of L sums to 1, $\vec{1}$ is an eigenvector with eigenvalue 1. Since L is a hermitian matrix, we know that its eigenvectors form an orthonormal basis for the space, and in particular that all of its other eigenvectors must oscillate so as to be orthogonal to $\vec{1}$. Now let's consider one of these other eigenvectors: on a hunch, let's look at

$$\vec{x} = \frac{1}{2} \begin{bmatrix} \cos\left(\frac{2\pi}{m}\right) \\ \vdots \\ \sin\left(\frac{2\pi m}{m}\right) \end{bmatrix}$$

What happens when we apply L to $\vec{x}$? Each entry of $\vec{x}$ becomes the average of its two neighboring entries. So, for example, the lth entry of $\vec{x}$ becomes

$$(L\vec{x})_l = \frac{1}{2}\left(\cos\left(\frac{2\pi(l-1)}{m}\right) + \cos\left(\frac{2\pi(l+1)}{m}\right)\right)$$

or by the standard rules of cosine addition,

$$(L\vec{x})_l = \cos\left(\frac{2\pi}{m}\right)\cos\left(\frac{2\pi l}{m}\right)$$

so

$$L\vec{x} = \cos\left(\frac{2\pi}{m}\right)\vec{x}$$

In other words, $\vec{x}$ is an eigenvector of L with eigenvalue $\cos\left(\frac{2\pi}{m}\right)$. That is, as the number of points goes to infinity, the eigenvector for L converges to *sin* with eigenvalue 1.

Note that by symmetry sin is also a perfectly good eigenfunction of L with the same eigenvalue. In fact, since our matrix L is Hermitian, its eigenvectors must all be orthogonal to each other. Since the trivial eigenvector is constant and positive, it follows that all other eigenvectors must oscillate. After finding that sin and cos are eigenvectors, it should come as no surprise that the others might look like

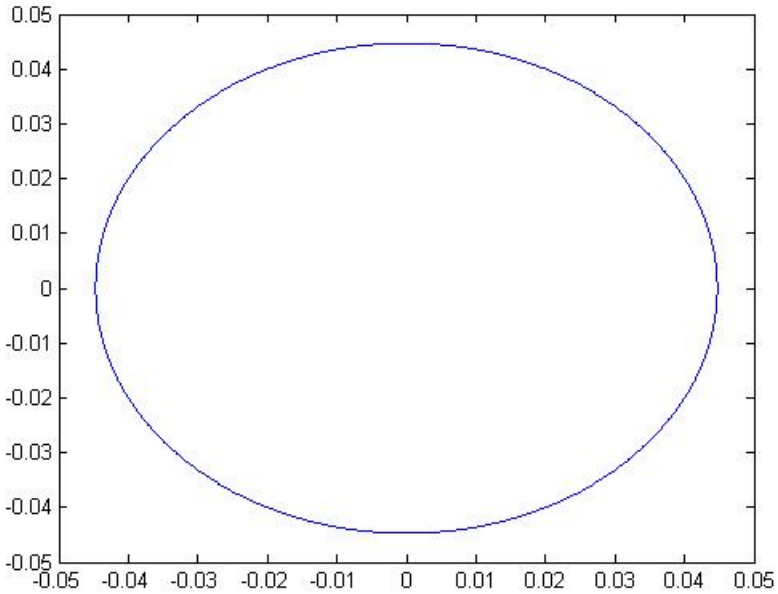

FIGURE 2.2. A nice circle in $\mathbb{R}^2$

$\sin(2\pi nx), \cos(2\pi nx)$. In fact, if we define the Laplacian as a mathematician would, with a negative sign,

$$\triangle = -\frac{d^2u}{dx^2}$$

then indeed the eigenvalues and vectors for L converge to those of the continuous Laplacian as our graph becomes continuous. This justifies our use of the term "Graph Laplacian."

Unfortunately, the eigenvector cos only works locally as a low-distortion mapping. For example, cos maps $x \in B_\epsilon(\frac{\pi}{2})$ onto the interval $[0, 1]$ with arbitrarily small distortion as $\epsilon \to 0$. But if we try to map the whole circle using cos, we find the distortion becomes infinite since cos maps $\frac{\pi}{2}$ and π both to 0. And indeed, the theorem only guarantees that we'll be able to map a d dimensional manifold to $\mathbb{R}^d$ for a small neighborhood around a given point. In order to map the entire circle into $\mathbb{R}$ with low distortion, we would have to do so in at least 4 separate segments (alternating the use of sin and cos). But if we aren't so picky about the dimension we map to, we can use these two eigenfunctions together to map the distorted circle in $\mathbb{R}^3$ onto a nice circle in $\mathbb{R}^2$.

3. Cryo-electron microscopy

3.1. **Statement of the Problem.** Cryo-electron microscopy provides an excellent example of a domain in which Laplacian eigenfunction maps are unexpectedly but nearly perfectly suited to the problem. Cryo-EM is a form of electron microscopy used to discover the shapes of proteins. It offers an alternative to the more well-known technique of x-ray crystallography in the case of proteins that are difficult or

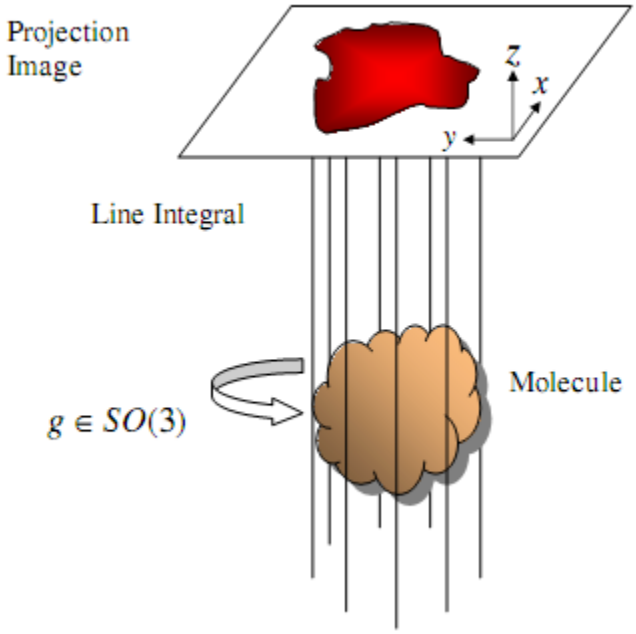

FIGURE 3.1. The cryo-EM experiment (figure courtesy of Singer [3]

impossible to crystallize without changing the shape of the protein. In cryo-EM, the protein being studied is frozen rapidly in a layer of ice, then imaged in an electron microscope. The experimenter has no control over the orientations of the molecules when they were crystallized. Nor can the experimenter image multiple times, for the proteins are so delicate that they are destroyed as the image is produced. The resulting image has a darkness in each pixel corresponding to the integral of the electric potential of the molecule (which is proportional to what we mean by the "shape" of the molecule) in the direction perpendicular to the image. That is,

$$P_g(x, y) = \int \phi_g(x, y, z)dz$$

where $\phi_g(x, y, z)$ is the electric potential of the molecule when the molecule is rotated by some rotation g. We can imagine these rotations in a number of ways; picturing them as random elements of the quaternions is likely to be less helpful for our purposes than imagining a vector pointing from the center of the unit sphere to a point on the surface that can indicate the orientation of the molecule, and a vector pointing somewhere on the unit circle that can indicate the rotation of the molecule with respect to its orientation vector.

The experimenter is left with a number of problems to solve before she can reconstruct the original shape of the molecule. The first is to figure out how the molecule was oriented in each image. The second is to use these projection images to reconstruct the original 3D shape. And the continual problem is the elimination of noise: in these images, the noise from stray electrons bouncing unpredictably off the interstitial ice and behaving erratically in general can be one hundred times

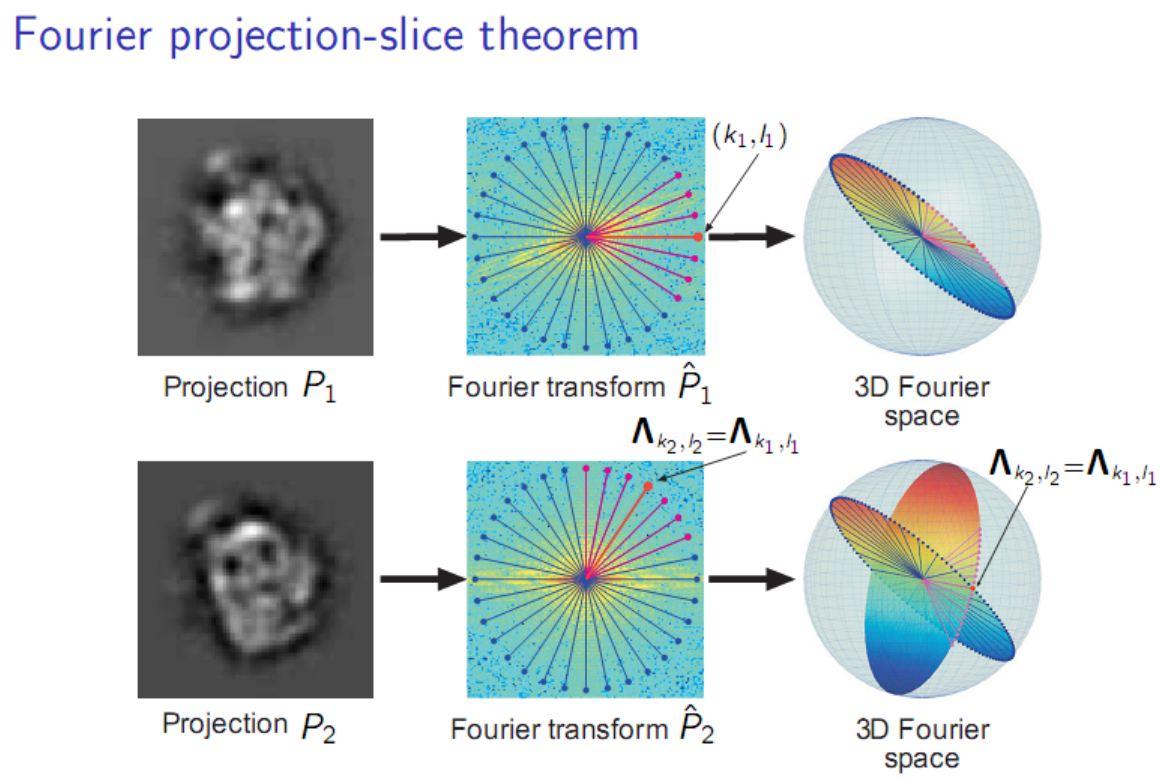

FIGURE 3.2. The Fourier Slice Theorem (figure courtesy of [3])

greater than the signal from the protein. I'll address the problems in order of their simplicity: first the reconstruction of the shape of the molecule from the properly oriented projection images, second the reorientation of the projection images into their proper order, and in the very distant future I'll begin to address the noise.

The zeroth step, though, is to reduce the noise and the complexity of the second step all at once. We match each image against each other image and if they look like rotations of each other, then we just take the average of the two images and use it instead. Thus we no longer need to worry about finding the rotation of the molecule on the unit circle, and reduce the problem to finding the correct orientation vector for the molecule on the unit sphere.

3.2. **The Fourier Slice Theorem.** Suppose that we have all the images and we know their proper orientations. Then it turns out that we can use the Fourier Slice Theorem to reconstruct the original molecule with relative ease. The algorithm is simple: take the 2D fourier transform of the projection images. The theorem tells us that each one of these 2D fourier images is a slice through the 3D fourier space for the molecule. So arrange the 2D fourier images properly in the 3D fourier space, and take the 3D inverse fourier transform to recover the original shape of the molecule. The proof of the Fourier Slice Theorem is included in the appendix.

3.3. **Reconstructing the 2-sphere.** The task, then, is to arrange the 2D fourier images properly within 3D fourier space. To do this, we will try to create a graph laplacian matrix for the two sphere in the same way that we previously did for the circle and find its eigenvalues. We discretize the space by decomposing each of the K images into L radial lines. Just as in the case of the circle, a graph laplacian that acts on a vector $\vec{x}$ by returning as the jth entry the average value of $\vec{x}$at the vertices neighboring j will have eigenvectors which converge to those of the continuous Laplacian on the 2 sphere in the limit as the number of radial lines goes to infinity.

In order to find the neighbors of each radial line, we imagine the 2D images in the 3D space and consider what we know about the relationships between the images. Each two images are planes through the 3D fourier space, and thus must intersect along exactly one line. The neighbors $\mathcal{N}(k,l)$ of a radial line (k,l) are the vertices just before and just after it on each of the images in which it appears. Thus, we say $(k',l') \in \mathcal{N}(k,l)$ if $(k,l) = (k',l' \pm 1)$. [1] We can imagine each set of neighbors $\mathcal{N}(k,l)$ as a spider whose body is the vertex (k,l). Then the graph laplacian is simply

$$A_{(k,l)(k',l')} = \begin{cases} \frac{1}{|\mathcal{N}(k,l)|} : & (k',l') \in \mathcal{N}(k,l) \\ 0 : & (k',l') \notin \mathcal{N}(k,l) \end{cases}$$

It is easy to see that the trivial eigenvector $\vec{1}$ will be an eigenvector of A with eigenvalue 1. More interesting is the fact that the coordinate vectors $\vec{x}, \vec{y}, \vec{z}$ are also eigenvectors of A. Simply observe that the center of mass of the spider around vertex (k,l) lies on the line between (k,l) and the origin. Also, the distance of the center of mass from the vertex depends only on the lengths of the spiders' legs, and not on the number of legs. Thus, it is the same for every vertex. Call it λ. Then we have shown

$$L\vec{x} = \lambda\vec{x}$$

$$L\vec{y} = \lambda\vec{y}$$

$$L\vec{z} = \lambda\vec{z}$$

Notice that $\vec{x}, \vec{y}, \vec{z}$ are eigenfunctions of the Laplacian on the 2 sphere — that is, they are the spherical harmonics $Y_l^m = 1$, just as the eigenvector $\vec{1} = Y_0^0$. It is not too much of a stretch to guess that the other eigenfunctions will converge to the other spherical harmonics as the number of points increases.

Once again, no one of these eigenvectors (or even two) will suffice to give us a low distortion mapping over the whole sphere. But mapping the terminus of each radial line (k,l) to the point $(\vec{x}, \vec{y}, \vec{z})_{kl}$ (and normalizing properly) we can fill up the volume of the sphere in the 3D fourier space. With a simple inverse fourier transform, we then obtain the original shape of the molecule.

This algorithm is remarkably robust - it is able to correctly find the shape of a molecule when the images contain 30 times as much noise as they do signal ([1]). Unfortunately, current techniques produce about 100 times more signal than noise. Research into increasing the robustness of the algorithm is ongoing.

[1] The set of neighbors of a radial line can be extended to the first m lines on either side of it in each image in which it appears, and extending the set can make the algorithm more robust to noise.

4. The general proof

Here I sketch the proof of the theorem stated above (1). For the full proof, see [2]. In what follows, $a \sim b \iff \exists C_1, C_2$ constants such that $a \leq C_1 b$ and $a \geq C_2 b$.

To begin the proof, note that we are looking for a set of d basis vectors that we can use to map a region of our d-dimensional manifold onto $\mathbb{R}^d$. We can use the spectral theorem to prove that the eigenfunctions of the Laplacian form such a complete set. The difficult thing is to show that with low distortion we can find a single eigenfunction of the Laplacian to use as each orthogonal coordinate in the mapping. In order to show that the mapping has low distortion, we want to show that

$$\partial_p \phi_j(z') \sim R_z^{-1}$$

where $R_z$is the radius of the region around z that we are mapping, so that the eigenfunction changes by order 1 over the region in the direction p. If we can pick such an eigenfunction for all linearly independent directions p, we will have found the low distortion mapping we were looking for.

4.1. **Lemmas.** Consider the heat kernel

$$K(z, z_0, t) = \sum_{j=1}^{\infty} \phi_j(z)\phi_j(z_0)e^{\lambda_j t} \tag{4.1}$$

Lemma 2. *Proposition 3.1.2 from Jones tells us that for w in an annulus of radius $\frac{\delta_0}{2} < r < \delta_0$ around z,*

$$\|K_t(z, w)\| \sim t^{\frac{-d}{2}}$$

and for p a unit vector in the direction of $z - w$,

$$\|\partial_p K_t(z, w)\| \sim t^{\frac{-d}{2}} \frac{R_z}{t} \tag{4.2}$$

which is proved by considering the heat kernel as the density of Brownian walkers that move from z to z_0 in time t.

Next we want to show that we can find a single eigenfunctions such that it has a large gradient in the p direction. We do this by first showing that by Weyl's bound

$$\#\{j : \lambda_j \leq \lambda\} \lesssim \mid \Omega \mid \lambda^{\frac{d}{2}} \tag{4.3}$$

we can throw out all the eigenfunctions with eigenvalues that are too big or too small. Furthermore, by using the pigeonhole principle along with Weyl's bound we can leave out eigenfunctions whose gradients in the p direction are too much smaller than their L^2 norms on the space. Let Λ be this set of good eigenfunctions. In fact,

Lemma 3. *For all $\phi_j \in \Lambda$ and for all z' such that $\|z - z'\| \lesssim \delta_0 R_z$*

$$\mid \partial_p \phi_j(z') \mid \sim R_z^{-1} \frac{1}{\mid B(z, \delta_0 R_z) \mid} \left(\int_{B(z, \delta_0 R_z)} \phi_j^2 \right)^{-\frac{1}{2}} \tag{4.4}$$

4.2. **Proof of Theorem 1.** Then all that remains is a simple proof by induction. Pick a direction p_1 at random. Then by (3), we can find $\phi_1$such that $\mid \gamma_1 \partial_{p_1} \phi_1(z) \mid \gtrsim R_z^{-1}$. Then for the induction, we suppose we've chosen directions $p_1, \ldots, p_k$ for $k < d$ and eigenfunctions $\phi_1, \ldots, \phi_k$ such that $\mid \gamma_i \partial_{p_i} \phi_i(z) \mid \gtrsim R_z^{-1}$ for all $i = 1, \ldots, k$. Then we pick $p_{k+1}$to be orthogonal to the gradients of all the preceding eigenfunctions chosen. By (3) we can find ϕ_{k+1}such that $\mid \gamma_{k+1} \partial_{p_{k+1}} \phi_{k+1}(z) \mid \gtrsim R_z^{-1}$. Thus we arrive at a set of d eigenfunctions whose gradients are both large and linearly independent of each other. One can show using the fundamental theorem of calculus that $\Phi(z') = (\gamma_1 \phi_1(z'), \ldots, \gamma_d \phi_d(z'))$ maps a ball around z into $\mathbb{R}^d$ with low distortion.

Appendix A. Appendix: Selected Proofs

A.1. **The Spectral Theorem.** We use the spectral theorem to show that the Laplacian has a spectral decomposition with a discrete spectrum.

Theorem 4. *The Spectral Theorem*

A bounded, compact operator $T : \mathcal{H} \to \mathcal{H}$ has a discrete spectrum $\lambda_1 \geq \lambda_2 \geq \ldots \geq \lambda_j \to 0$,

$$T\phi_j = \lambda_j \phi_j$$

such that its eigenfunctions ϕ_j are all orthonormal and there are only a finite number of eigenvalues λ_j in any interval.

Consider the inverse Laplacian $\triangle^{-1}$:

$$\triangle f = g \iff \triangle^{-1} g = f$$

We can write the inverse Laplacian as a Green's function.

$$f(z) = (\triangle^{-1} g)(z) = \int_{-\infty}^{\infty} G(z, w) g(w) dw$$

It so happens that the Green's function for the Laplacian is just the integral of the heat kernel:

$$G(z, w) = \int_0^{\infty} K_t(z, w) dt$$

And we can easily show using this formula and the Cauchy-Schwartz Lemma that $\triangle^{-1}$ is a bounded, compact, Hermitian operator, so that its eigenfunctions form a . Then letting the eigenvalues and eigenfunctions of $\triangle^{-1}$ be Λ_j, ϕ_j, we have

$$\begin{aligned} \triangle^{-1} \phi_j = \Lambda_j \phi_j &\iff \phi_j = \Lambda_j \triangle \phi_j \\ &\iff \frac{1}{\Lambda_j} \phi_j = \triangle \phi_j \end{aligned}$$

Thus the ϕ_j are eigenfunctions of the Laplacian with eigenvalues $\lambda_j = \frac{1}{\Lambda_j}$, and they must form an orthonormal basis for the space.

A.2. **Fourier slice theorem.** We prove the Fourier slice theorem in two dimensions.

Theorem 5. *Fourier Slice Theorem:*
Let $f(x,y)$ be a two dimensional function and $F(k_x,k_y)$ its fourier transform. Then the slice of the two dimensional fourier space through the origin along the x axis is just the fourier transform of the projection $p(x)$ of f(x,y) along the x axis. That is,

$$\int_{-\infty}^{\infty} p(x)e^{-2\pi i x k_x}dx = F(k_x,0) \tag{A.1}$$

Proof. We define

$$p(x) = \int_{-\infty}^{\infty} f(x,y)dy$$

and

$$F(k_x,k_y) = \int_{-\infty}^{\infty}\int_{-\infty}^{\infty} f(x,y)e^{-2\pi i(xk_x+yk_y)}dxdy$$

Then

$$\begin{aligned} F(k_x,0) &= \int_{-\infty}^{\infty}\int_{-\infty}^{\infty} f(x,y)e^{-2\pi i x k_x}dxdy \\ &= \int_{-\infty}^{\infty}\left[\int_{-\infty}^{\infty} f(x,y)dy\right]e^{-2\pi i x k_x}dx \\ &= \int_{-\infty}^{\infty} p(x)e^{-2\pi i x k_x}dx \end{aligned}$$

□

The proof for dimension greater than two is only notationally more complex.

A.3. **Weyl's lemma.** We will prove Weyl's Lemma for the case of a Euclidean doman Ω in two dimensions with Dirichelet boundary conditions (that is, solutions to Laplace's equation are constrained to be zero at the boundary).

Lemma 6. *Weyl's Lemma:*
For any $T > 0$,

$$\#\{j : 0 < \lambda_j \leq T\} \leq CT \mid \Omega \mid \tag{A.2}$$

for some constant C.

Proof. We let $K^{\Omega}(x,x',t)$ be the heat kernel on Ω, and $K^{\mathbb{R}^2}(x,x',t)$ be the Euclidean heat kernel: the heat kernel on $\mathbb{R}^2$. We can think of the Euclidean heat kernel as a special case of Dirichelet boundary conditions in which the boundary is sent to infinity. Hence we can think of $K^{\Omega}(x,x',t)$ as being a deformation of $K^{\mathbb{R}^2}(x,x',t)$ in which we squeeze in the zeros from infinity.

Alternatively, one can interpret the heat kernel $K^{\Omega}(x,x',t)$ as the density of brownian walkers leaving x at time 0 and arriving at x' at time t without hitting the (absorbing, Dirichelet) boundary. Since the brownian walkers in $\mathbb{R}^2$ can never hit the boundary and never be absorbed, it is clear that

$$\int_\Omega K^\Omega(x,x,t)dA(x) \leq \int_\Omega K^{\mathbb{R}^2}(x,x,t)dA(x) \tag{A.3}$$

Now, on the left hand side the heat kernel on Ω can be written in terms of the Laplacian eigenfunctions

$$\begin{aligned}\int_\Omega K^\Omega(x,x,t)dA(x) &= \int_\Omega \sum_j \phi_j(x)\phi_j(x)e^{-\lambda_j t}dA(x)\\ &= \sum_j \left({}_j\int_\Omega \phi_j(x)\phi_j(x)dA(x)\right) e^{-\lambda_j t}\\ &= \sum_j e^{-\lambda_j t}\end{aligned}$$

if the eigenfunctions are properly normalized. On the right hand side, we know that the Euclidean heat kernel is just a gaussian centered at x. Then for some constant c (depending on the dimension of Ω),

$$\begin{aligned}\int_\Omega K^{\mathbb{R}^2}(x,x,t)dA(x) &= \int_\Omega ct^{-1}e^{-\frac{x^2}{4t}}dA(x)\\ &= ct^{-1}\int_\Omega dA(x)\\ &= ct^{-1} \mid \Omega \mid\end{aligned}$$

Since $e^{-\frac{x^2}{4t}} \leq 1$. Thus we have

$$\sum_j e^{-\lambda_j t} \leq ct^{-1} \mid \Omega \mid$$

$$\sum_{0<\lambda_j\leq T} e^{-\lambda_j t} \leq ct^{-1} \mid \Omega \mid$$

Fix $t = T^{-1}$and note that $0 \leq \frac{\lambda_j}{T} \leq 1$, so

$$\sum_{0<\lambda_j\leq T} e^{-\lambda_j t} \leq cT \mid \Omega \mid$$

$$\sum_{0<\lambda_j\leq T} e^{-1} \leq cT \mid \Omega \mid$$

$$\#\{j : \lambda_j \leq T\} \leq CT \mid \Omega \mid$$

for $C = ec$. □

The proof for dimension greater than two is similar.

A.4. **Convergence of the graph laplacian.** In this paper I showed in two examples that the eigenvalues and functions of the averaging operator, or graph laplacian, on the graph converge to those of the continuous Laplacian operator on the manifold as the number of points goes to infinity. Here I present another justification for the same phenomenon. For notational simplicity I remain in two dimensions.

Let F be a function in $L^2$and let $F_x(z)$denote the partial derivative of F at z with respect to x.

Let $A_r$be an averaging operator, so $A_r(F) = \frac{1}{Vol(B(z_0,r))}\int_{B(z_0,r)} F(z)dz$. Then by Taylor expanding F we find that

$$A_r(F)\mid_{z_0} = \frac{1}{Vol(B(z_0,r))}\int_{B(z_0,r)} [F(z_0)+xF_x(z_0)+yF_y(z_0)+x^2F_{xx}(z_0)+y^2F_{yy}(z_0)+2xyF_{xy}(z_0)+O(r^3)]dz$$

The odd terms integrate to zero, so

$$A_r(F)\mid_{z_0} = \frac{1}{Vol(B(z_0,r))}\int_{B(z_0,r)} [F(z_0)+x^2F_{xx}(z_0)+y^2F_{yy}(z_0)+O(r^3)]dz$$

Since the volume goes like cr^d,

$$A_r(F)\mid_{z_0} = F(z_0)+cr([F_{xx}(z_0)+F_{yy}(z_0)]+O(r^3)$$

$$F_{xx}(z_0)+F_{yy}(z_0) = \frac{A_r(F)\mid_{z_0} -F(z_0)+O(r^3)}{cr}$$

if the higher order derivatives of F are not too large, then

$$\triangle(F(z_0)) = \lim_{r\to 0}\frac{I-A_r}{cr}(F(z_0))$$

$$\triangle = \lim_{r\to 0}\frac{I-A_r}{cr}$$

or in general

$$\triangle = \lim_{r\to 0}\frac{I-A_r}{cr^{\frac{d}{2}}}$$

So indeed the eigenvectors of $\triangle$should converge to those of the averaging operator as the radius over which we average gets small if we normalize properly. Notice that subtracting off the identity operator is equivalent to averaging over the neighbors of a point but not the point itself — which is just how we constructed the averaging operator for the circle and for cryo-EM.

References

1. R. Coifman, A. Singer, Y. Shkolnitsky, and F. Sigworth, *Cryo-em structure determination through eigenvectors of sparse matrices*, Tech. Report YALEU/DCS/TR-1389, Yale University, 2009.
2. P. W. Jones, M. Maggioni, and R. Schul, *Universal Local Parametrizations via Heat Kernels and Eigenfunctions of the Laplacian*, Proc. Nat. Acad. Sci **105** (2008), no. 6.
3. A. Singer, *Cryo-electron microscopy and data organization through eigenvectors of sparse operators*, IPAM CDI Workshop, October 2007.

Yale University, New Haven, CT
E-mail address: madeleine.udell@aya.yale.edu